Journal of Nuclear Materials 386–388 (2009) 768–771

Contents lists available at ScienceDirect

Journal of Nuclear Materials

journal homepage: www.elsevier.com/locate/jnucmat

Hydrogen behavior in damaged tungsten by high-energy ion irradiation

M. Fukumoto [a,*], H. Kashiwagi [a], Y. Ohtsuka [a], Y. Ueda [a], Y. Nobuta [b], J. Yagyu [c], T. Arai [c], M. Taniguchi [c], T. Inoue [c], K. Sakamoto [c]

[a] Graduate School of Engineering, Osaka University, 2-1 Yamadaoka, Suita, Osaka 565-0871, Japan
[b] Laboratory of Plasma Physics and Engineering, Hokkaido University, Kita-13, Nishi-8, Kita-ku, Sapporo 060-8628, Japan
[c] Japan Atomic Energy Agency, 801-1 Mukoyama, Naka, Ibaraki 311-0193, Japan

A B S T R A C T

Effects of radiation damage on the behavior of hydrogen trapped in tungsten were investigated using a mixed hydrogen–carbon ion beam and deuterium ion beam. Radiation damage was produced by 300 and 700 keV negative hydrogen ion beams. The number density of blisters formed on the radiation-damaged samples was less than an undamaged sample. SIMS measurements showed that post-implanted deuterium was mainly trapped at radiation damage sites. These results suggest that hydrogen accumulation at the grain boundaries is greatly decreased due to significant trapping of hydrogen isotopes at radiation damage sites.

1. Introduction

Tungsten is a promising candidate for plasma facing materials (PFMs) for future fusion devices. In D–T fusion reactors, the PFMs are irradiated with energetic deuterium and tritium ions. Therefore, studies on hydrogen isotope irradiation were performed using ion beam irradiation devices or plasma simulators. These studies clarified hydrogen behavior in tungsten such as surface morphology, hydrogen isotope retention and release, and depth distribution of hydrogen isotopes [1–4]. Moreover, the effects of carbon impurities on the hydrogen isotope behavior in tungsten were also investigated by pre-irradiation or simultaneous irradiation of a carbon ion beam [5–7]. However, these results did not include the influence of radiation damage.

The PFMs are also irradiated with 14 MeV neutrons, which produce radiation damage. Thus, it is important to investigate the behavioral characteristics of hydrogen isotopes, which include surface morphology, retention, and distribution in radiation-damaged PFMs for safe and stable operations. Hydrogen isotope retention in radiation-damaged tungsten was investigated in previous studies [8,9]. Haasz et al. showed that deuterium retention in tungsten increased with cumulative fluences [8]. Deuterium retention and release from 800 MeV proton irradiated and annealed tungsten were investigated by Oliver et al. [9]. He reported that post-irradiated deuterium was trapped in 1.4 eV traps. However, the surface morphology and deuterium distribution in radiation-damaged tungsten are not clear.

In this study, the effects of radiation damage on the surface morphology and deuterium distribution in radiation-damaged tungsten were investigated using a mixed hydrogen–carbon and deuterium ion beam. The radiation damage was produced by a high-energy negative hydrogen ion beam.

2. Experimental

Polycrystalline tungsten sheets with a purity of 99.99 at.% fabricated by A.L.M.T Corp. were used in this study. To relieve internal stresses, the tungsten sheets were annealed at 1173 K for 0.5 h in a hydrogen atmosphere after being hot rolled to 1 mm thickness. Tungsten samples (20 × 10 mm) were cut from these sheets. The sample surfaces were mirror-polished mechanically to a roughness of less than 0.1 μm.

Radiation damage was produced by a high-energy negative hydrogen ion beam in the MeV Test Facility [10] at the Japan Atomic Energy Agency. The ion beam energies were 300 and 700 keV. In the case of the 300 keV H^- beams, since the mean depth of radiation damage and the depth of the first grain boundaries are comparable, some first grain boundaries exist in the radiation-damaged zone, but others do not. In the case of the 700 keV H^- beams, however, most first grain boundaries exist in the radiation-damaged zone. To reduce oxygen impurities in the ion beam, a cesium oven in the ion source was heated. The tungsten samples were fixed to a water-cooled calorimeter using a sample holder made of copper. Carbon sheets were inserted between the samples and the sample holder to increase the heat conductivity and prevent temperature increases during high-energy H^- beam irradiation. To prevent radiation damage from recovering, ion beam irradiation was

* Corresponding author. Tel.: +81 6 6877 5111/3309; fax: +81 6 6879 7867.
E-mail address: fukumoto@st.eie.eng.osaka-u.ac.jp (M. Fukumoto).

0022-3115/$ - see front matter © 2008 Elsevier B.V. All rights reserved.
doi:10.1016/j.jnucmat.2008.12.213

performed repeatedly for ~1 s every 60 s, and the sample temperature, which was measured by a pyrometer, was maintained below 473 K.

To form blisters, the mixed H^+–C^+ beam was post-irradiated using a High Flux Irradiation Test device (HiFIT) [7,11,12]. Post-irradiation was performed under the ITER-FEAT first wall conditions. The beam energy, flux, and sample temperature were 1.0 keV, $\sim 2.2 \times 10^{20}$ H^+/m^2s, and 473 K, respectively. The hydrogen atom species ratios irradiated on samples were 70%, 10%, and 20% for 0.3, 0.5, and 1.0 keV H, respectively. According to Behrisch et al. [13], the first walls were irradiated with the charge-exchange neutrals and ions with energies of ~600 and ~300 eV ($3kT_e + 2kT_i$), respectively. The total flux of these particles was on the order of 10^{19}–10^{20} atoms/m^2s. During operation, since blanket modules are cooled by water at a temperature of 373–423 K [14], the temperature of the first wall would be higher than that of the cooling water. Therefore, the experimental conditions match well with the ITER-FEAT first wall conditions. The fluence was $\sim 7.5 \times 10^{24}$ H^+/m^2. In order to generate blisters even at low fluences, carbon ions were simultaneously irradiated on the samples. The carbon ion concentration in the hydrogen ion beam was ~0.8%. According to a previous study [7], carbon impurities of about 1.0% in the H^+ beam produce a WC layer on a sample surface. This layer reduces the hydrogen recombination rate on the surface, which helps to prevent implanted hydrogen from escaping from the surface.

To obtain the effects of radiation damage on hydrogen isotope trapping, D^+ beam was post-implanted to radiation-damaged samples. The beam energy, flux, fluence, and sample temperature were 1.0 keV, $\sim 1.6 \times 10^{20}$ D^+/m^2s, $\sim 5.0 \times 10^{23}$ D^+/m^2, and 473 K, respectively. Deuterium atom species ratios irradiated on samples were 50%, 30%, and 20% for 0.3, 0.5, and 1.0 keV D, respectively.

The surface morphology of post-irradiated samples was observed using a scanning electron microscope (SEM). The cross-sections of blisters formed on samples were obtained using focused ion beam (FIB) devices with a 30 keV gallium ion beam. Depth profiles of post-implanted deuterium were analyzed by secondary ion mass spectroscopy (SIMS) with the primary ion beam of Cs^+ at an incident angle of 60° from the surface normal. The beam energy and current of the primary ion beam were 11 keV and 200 nA, respectively. To obtain secondary ions (D^-) from a flat crater, a focused Cs^+ beam was scanned over a 300×300 μm^2 area. The D^- signal was detected from the center of 6% of the sputtered crater. The depth of the sputtered crater was determined using a surface profilometer.

3. Results and Discussion

Fig. 1 shows the surface morphology of (a) an undamaged sample, (b) a sample damaged by 300 keV H^- to 3.7 dpa and (c) a sample damaged by 700 keV H^- to 3.5 dpa. The value of dpa was defined as that at the maximum value. The undamaged sample was not pre-irradiated by the high-energy H^- beam. As shown in Fig. 1(a), small blisters of a few micrometer in diameter were formed on the undamaged sample. For the 300 keV H^- damaged sample (Fig. 1(b)), small blisters of a few micrometer in diameter were still formed, although the number of blisters was decreased. In the case of the 700 keV H^- damaged sample (Fig. 1(c)), almost all of the small blisters disappeared.

Fig. 2 shows the number density of blisters formed on the three samples (Fig. 1). As shown in Fig. 2, blisters with 20 μm in diameter were formed primarily on the undamaged sample. The 300 keV H^- damaged sample still had blisters with diameters less than 20 μm, although there were fewer than on the undamaged sample. In the case of the 700 keV H^- damaged sample, blisters with diameters less than 20 μm disappeared.

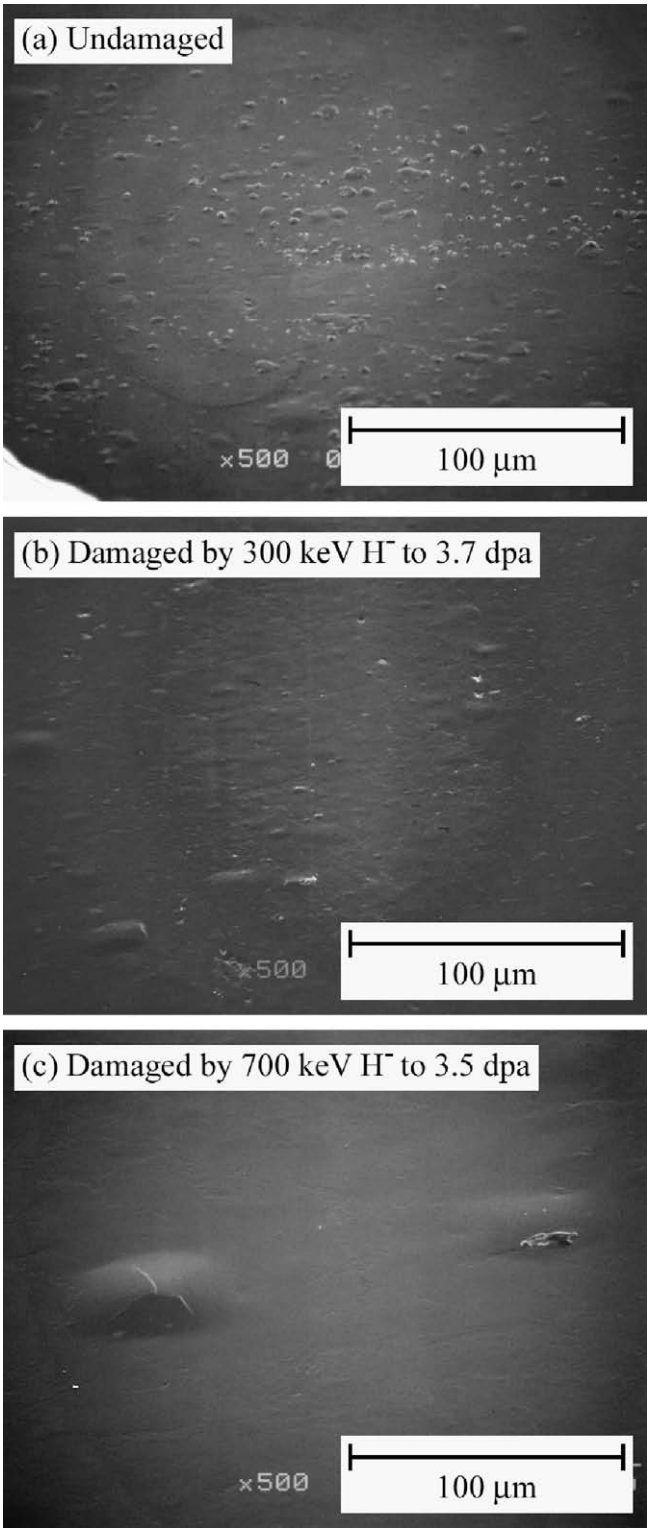

Fig. 1. Surface morphology of samples post-irradiated by mixed H^+–C^+ beam: (a) undamaged sample, (b) sample damaged by 300 keV H^- to 3.7 dpa and (c) sample damaged by 700 keV H^- to 3.5 dpa.

Fig. 3 shows the depth profiles of post-implanted deuterium in three samples: (a) top surface and (b) sub surface. The damage distributions estimated by TRIM-88 [15] are also shown in Fig. 3(c). As shown in Fig. 3(a), all three samples had a peak around the range of 0.3 keV for deuterium ions (~5 nm). At the sub surface, the deuterium concentration in the undamaged sample was very low, and its

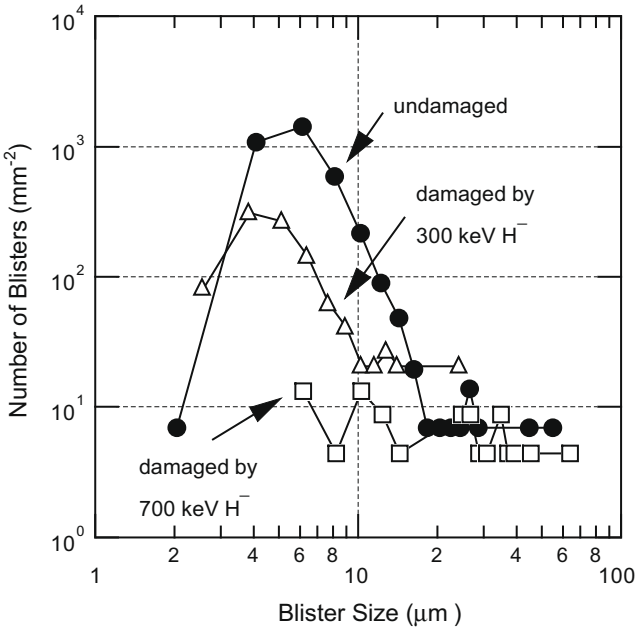

Fig. 2. Blister size distribution with damage energy as a parameter.

distribution was constant within the observed area. In the case of the samples damaged by 300 and 700 keV H^- beams, the deuterium concentration had a peak around ~0.2 μm deep. Beyond ~0.2 μm, the deuterium concentration decreased in both samples. It was shown that the accumulation of post-implanted deuterium in the radiation-damaged zone was more significant than in the undamaged sample. Beyond the radiation-damaged zone, the deuterium concentration of the radiation-damaged samples was similar to that of the undamaged sample. From these observations, it was found that the post-implanted deuterium diffused in the tungsten samples and was trapped in the radiation-damaged zone.

A cross-sectional view of a blister formed on tungsten irradiated with a mixed H^+–C^+ beam at 673 K is shown in Fig. 4. Using FIB devices, we obtained a cross-section of blisters without plastic deformation. Note that a gallium and tungsten co-deposition layer with a column structure was formed mainly on the upper side of the gap surface. It can be seen that a blister with a diameter of ~25 μm had a blister gap at a depth of ~5 μm. From other blisters including a result from Haasz et al. [8], we obtained the relationship between the blister diameter and the depth of blister gaps, shown in Fig. 5. The dashed and solid lines show the mean depth of radiation damage produced by the 300 and 700 keV H^- beams, respectively. As shown in Fig. 5, the depth of blister gaps increases with the blister diameter. The ratio of the blister diameter to the depth of the blister gaps is in the range of 0.1–0.2. Accordingly, blisters with diameters of 20 μm or less, which disappeared from the 700 keV H^- damaged sample, had blister gaps within 2–4 μm in depth. This depth agrees with the mean depth of radiation damage produced by a 700 keV H^- beam (~3.3 μm). These results indicated that the amount of hydrogen trapped at the grain boundaries may have decreased in the radiation-damaged zone.

In the case of the 300 keV H^- damaged sample, blisters with less than ~20 μm in diameter still formed, although their number decreased. The 300 keV H^- beam produced radiation damage to about ~1.1 μm, and the sample's first grain boundaries were within ~2 μm. When radiation damage does not reach the first grain boundaries, post-irradiated hydrogen accumulated at the first grain boundaries, leading to blister formation. However, when the radiation damage is produced around the first grain boundaries, blister formation was suppressed. This could be also due to a decrease of the accumulation of hydrogen at grain boundaries in the radiation-damaged zone.

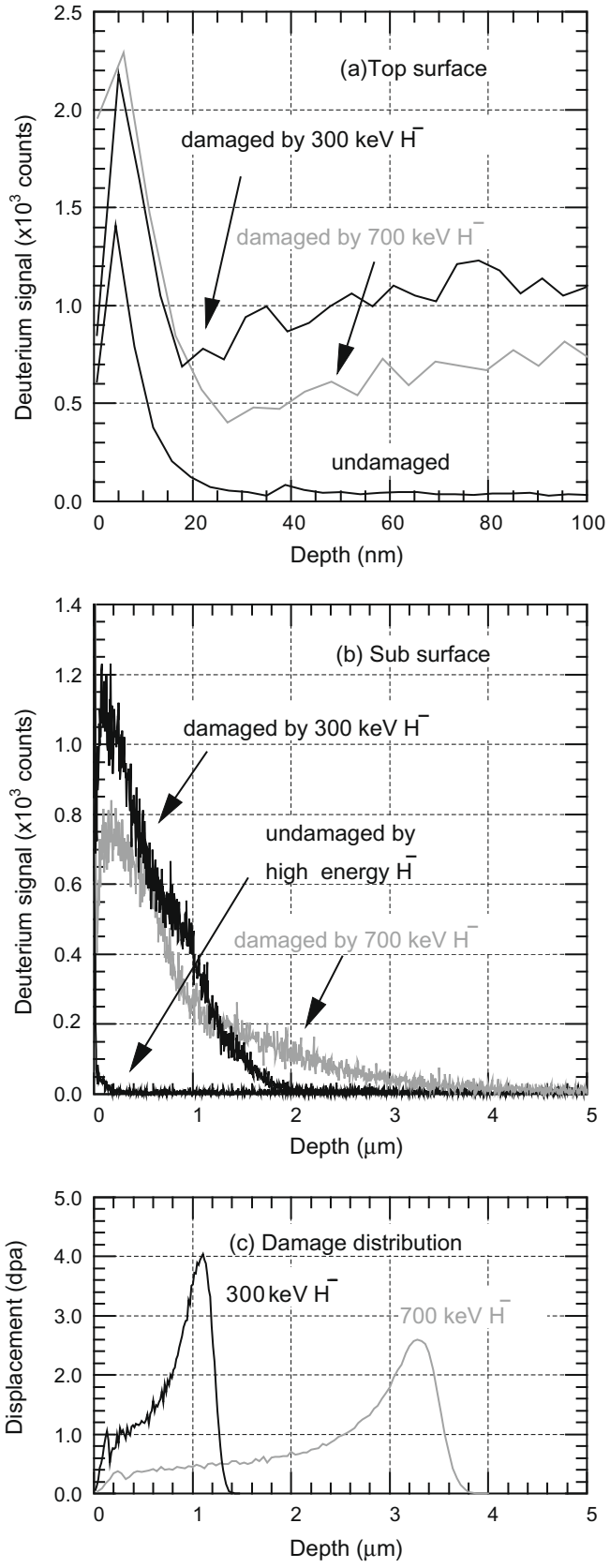

Fig. 3. Depth profiles of post-implanted deuterium analyzed by SIMS: (a) top surface, (b) sub surface, and (c) damage distributions estimated by TRIM-88 [15].

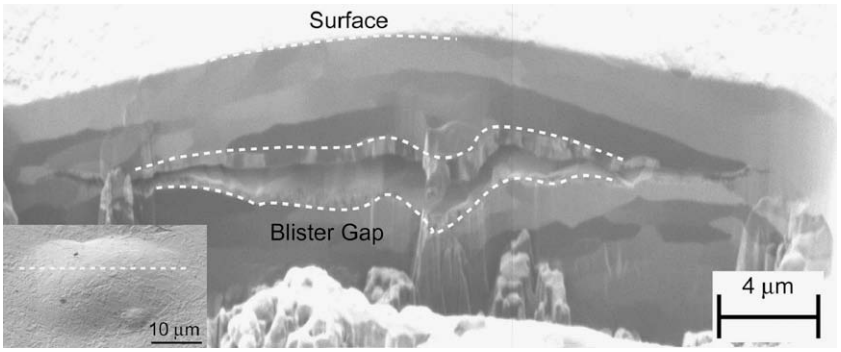

Fig. 4. Photograph obtained by FIB of a blister gap formed by irradiation of tungsten by a mixed H^+–C^+ beam at 653 K. Grains with different crystal orientations are indicated by variations in the brightness.

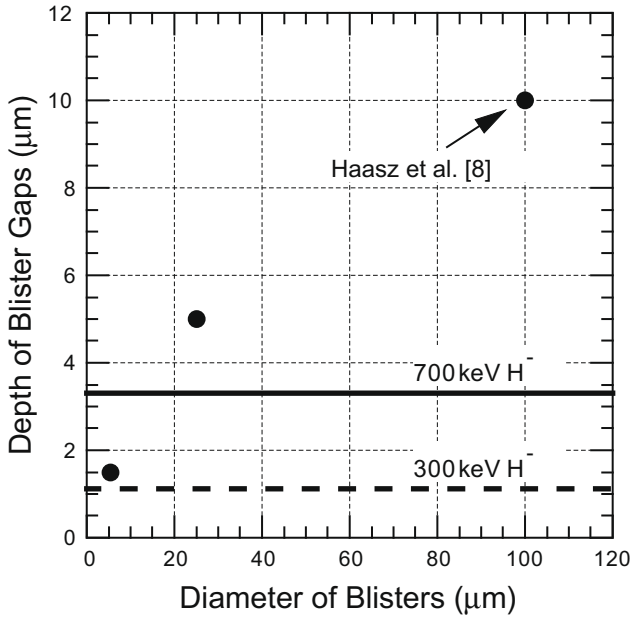

Fig. 5. Relationship between the blister diameter and the depth of the gap formed. The dashed and solid lines show the mean depth of radiation damage produced by the 300 and 700 keV H^- beams, respectively.

4. Conclusions

The effects of radiation damage on hydrogen trapping in tungsten were investigated. The radiation damage was produced by 300 and 700 keV negative hydrogen ion beams. After the damage creation, a 1 keV mixed hydrogen–carbon and deuterium ion beam irradiated the samples. The surface morphology of the post-irradiated samples and the cross-sections of blisters were observed by SEM and FIB, respectively. The deuterium depth distribution in the post-implanted samples was measured by SIMS.

It was shown that blisters with diameters less than 20 μm did not appear on the 700 keV H^- damaged sample. Blisters with diameters less than 20 μm had blister gaps within 2–4 μm deep. According to TRIM calculations, radiation damage was produced to a depth of about ~3.3 μm by the 700 keV H^- beam. SIMS analysis showed that post-implanted deuterium accumulated in this radiation-damaged zone. These results indicated that trapping of post-irradiated hydrogen isotopes at grain boundaries decreased due to trapping at radiation-damaged sites, and consequently blister formation was suppressed.

For the 300 keV H^- damaged sample, it was shown that the blisters with diameters less than 20 μm formed, although they were fewer than on the undamaged sample. Since the radiation-damaged zone (within ~1.1 μm) and the depth of the first grain boundaries (within ~2 μm) are comparable, some first grain boundaries exist in the radiation-damaged zone, but others do not. When the first grain boundaries are positioned beyond the radiation-damaged zone, small blisters with diameters of 20 μm or less formed. On the other hand, when the grain boundaries are positioned within the radiation-damaged zone, small blisters with diameters of 20 μm or less did not form. Therefore, small blisters less than 20 μm in diameter were decreased on the 300 keV H^- damaged sample.

Acknowledgment

One of the authors (M. Fukumoto) was provided financial support by "Kansai Research Foundation for technology promotion" for participation in the 13th International Conference on Fusion Reactor Materials (ICFRM-13).

References

[1] W. Wang, J. Roth, S. Lindig, C.H. Wu, J. Nucl. Mater. 299 (2001) 124.
[2] A.A. Haasz, J.W. Davis, M. Poon, R.G. Macaulay-Newcombe, J. Nucl. Mater. 258–263 (1998) 889.
[3] R.A. Causey, J. Nucl. Mater. 300 (2002) 91.
[4] R.A. Anderl, R.J. Pawelko, S.T. Schuetz, J. Nucl. Mater. 290–293 (2001) 38.
[5] V.Kh. Alimov, K. Ertl, J. Roth, K. Schmid, J. Nucl. Mater. 282 (2000) 125.
[6] M. Poon, J.W. Davis, A.A. Haasz, J. Nucl. Mater. 283–287 (2000) 1062.
[7] Y. Ueda, T. Shimada, M. Nishikawa, Nucl. Fusion 44 (2004) 62.
[8] A.A. Haasz, M. Poon, J.W. Davis, J. Nucl. Mater. 266–269 (1999) 520.
[9] B.M. Oliver, T.J. Venhaus, R.A. Causey, F.A. Farner, S.A. Maloy, J. Nucl. Mater. 307–311 (2002) 1418.
[10] T. Inoue, M. Taniguchi, T. Morishita, M. Dairaku, M. Hanada, T. Imai, M. Kashiwagi, K. Sakamoto, T. Seki, K. Watanabe, Nucl. Fusion 45 (2005) 790.
[11] T. Shimada, Y. Ueda, A. Sagara, M. Nishikawa, Rev. Sci. Instrum. 73 (2002) 1741.
[12] T. Shimada, H. Kikuchi, Y. Ueda, A. Sagara, M. Nishikawa, J. Nucl. Mater. 313–316 (2003) 204.
[13] R. Behrisch, G. Federici, A. Kukushkin, D. Reiter, J. Nucl. Mater. 313–316 (2003) 388.
[14] W. Dänner, A. Cardella, K. Ioki, R. Mattas, Y. Ohara, Y. Strebkov, Fusion Eng. Des. 55 (2001) 205.
[15] W. Eckstein, Computer Simulation of Ion–Solid Interaction, Springer Series in Material Science, vol. 10, Springer, Berlin, 1991.